REPORT 1367

CALCULATED AND MEASURED STRESSES IN SIMPLE PANELS SUBJECT TO INTENSE RANDOM ACOUSTIC LOADING INCLUDING THE NEAR NOISE FIELD OF A TURBOJET ENGINE [1]

By Leslie W. Lassiter and Robert W. Hess

SUMMARY

Flat 2024–T3 aluminum panels measuring 11 inches by 13 inches were tested in the near noise fields of a 4-inch air jet and turbojet engine. The stresses which were developed in the panels are compared with those calculated by generalized harmonic analysis. The calculated and measured stresses were found to be in good agreement.

In order to make the stress calculations, supplementary data relating to the transfer characteristics, damping, and static response of flat and curved panels under periodic loading are necessary and were determined experimentally. In addition, an appendix containing detailed data on the near pressure field of the turbojet engine is included.

INTRODUCTION

The problem of structural vibration due to acoustic loading has steadily become more severe particularly because of the widespread use of turbojet engines. Large areas such as wing and fuselage surfaces of the aircraft are exposed to intense random pressure fluctuations. These pressure fluctuations may induce many millions of loading cycles in a single flight and can thus cause fatigue of panels and secondary structure.

One of the prime needs in this problem is a means of determining, in the design stage, the magnitude of stresses that will be encountered by a given panel. The present paper, therefore, is concerned with the evaluation of the merits of a power-spectrum approach suggested by Miles as a means of predicting panel stresses. A family of simple test panels ranging in thickness from 0.032 inch to 0.081 inch was tested in the near sound field of an afterburner-equipped turbojet engine. These tests are an extension of reference 1 in that experimental and calculated stresses due to higher acoustic loadings are compared.

The presentation in reference 2 has been extended by a more complete description of the techniques used in obtaining calculated stresses. Also, because the calculation of stress for a given panel requires knowledge of the acoustic pressure loading and because very little data of this type are available in the literature, an appendix giving some detailed information on the near-field noise characteristics of the engine is included.

SYMBOLS

ω	frequency
ω_0	damped natural frequency
$Z(\omega)$	impedance of panel at frequency ω
$\Phi_N(\omega)$	power spectrum of noise input
$\Phi_N(\omega_0)$	power spectral density of noise at frequency ω_0
$\Phi_\sigma(\omega)$	power spectrum of stress response
$\overline{\sigma^2}$	mean-square stress
$\sqrt{\overline{\sigma^2}}$	root-mean-square stress
σ_{max}	stress amplitude
σ_{st}	static stress, positive in compression
S_0	static stress per unit static pressure
δ	damping as fraction of critical damping
p_1	root-mean-square acoustic siren pressure, psi
D	jet tailpipe diameter
z	axial distance from engine exit plane along lines 15° off jet center line
p	overall sound pressure, psi or dynes/cm²
d	distance from jet 15° boundary
R	radius of curved panels
$db = 20 \log_{10}\left(\dfrac{p}{0.0002}\right)$ where p is in dynes/cm²	
t	thickness

APPARATUS

PANEL CONFIGURATIONS

Flat panel.—In this investigation the response of both flat and curved panels was studied. The tests were made on 2024–T3 aluminum panels with thicknesses of 0.032 inch, 0.040 inch, 0.064 inch, and 0.081 inch. The flat panels had overall dimensions of 11 inches by 13 inches and were attached to a rigid 1-inch-thick aluminum plate by round-head bolts. The main features of this configuration are shown in figure 1 (a). The use of the rigid frame for mounting the panels avoided the additional complications which might arise from support flexibility. The bolt fastening was used to facilitate the attachment of panels to the mounting frame.

Curved panels.—For the tests with curved panels, the configurations consisted of flat panels rolled to the desired radius of 4 feet and mounted on a curved steel frame of the same radius. As shown in figure 1 (b), this frame was attached to the same type of rigid aluminum plate as was used for the

(a) Flat panel.
(b) Curved panel.

FIGURE 1.—Details of test panels.

(a) Laboratory mounting.   (b) Field mounting.

FIGURE 2.—Panel mounts used in tests.
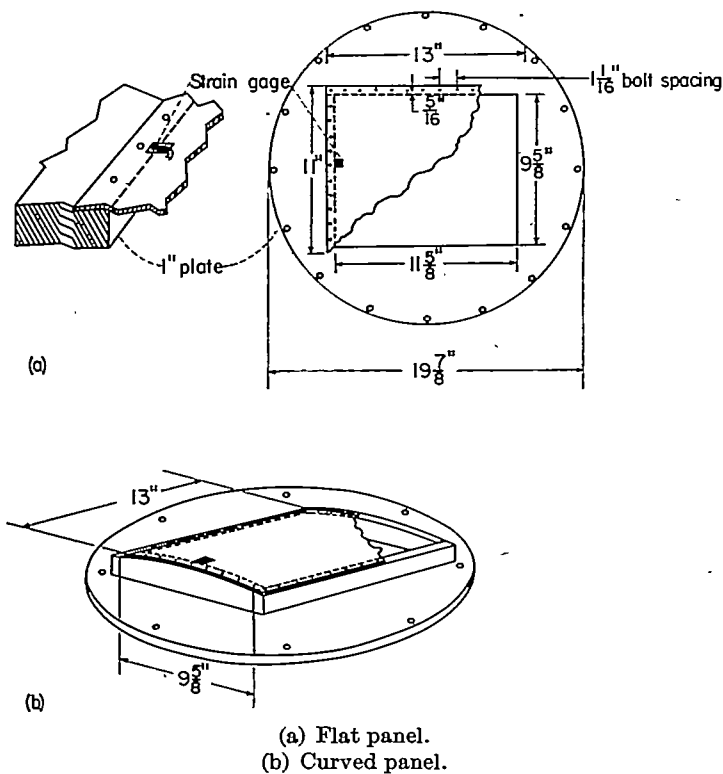
flat panels. The panel attachment to the frame was identical to that used with flat panels.

PANEL-MOUNTING CONDITIONS

Laboratory mounting.—The tests were divided into two parts—laboratory tests and field tests. Figure 2 shows schematically the two mounting conditions employed in the tests. Figure 2 (a) shows the laboratory mounting which consisted of a steel chamber, 18 inches in diameter and 12 inches deep, with a flange on the open end to permit attachment of the panel mounting plate. This chamber was convenient for applying either a positive or a negative pressure to the back side of the panel so that its static characteristics could be studied. During the laboratory tests this chamber behind the panels was filled with a porous material having rather poor sound-absorbing properties.

Field mounting.—Figure 2 (b) shows schematically the field mounting used for tests in the near sound field of a turbojet engine. The panel was mounted flush with a plywood surface in an attempt to simulate the acoustic environment of an isolated panel in a large reflecting surface. The backing chamber for this mount was also of plywood and had roughly twice the volume of that of the laboratory mount. This volume was filled to about 80 percent of its capacity with glass wool, which is more sound absorptive than the material used for the laboratory mount. Because this difference in mounting and backing or both was found to have a large effect on the panel damping, the terms "laboratory mount" and "field mount" will be used to differentiate between the test conditions throughout the report.

DISCRETE-FREQUENCY NOISE GENERATOR

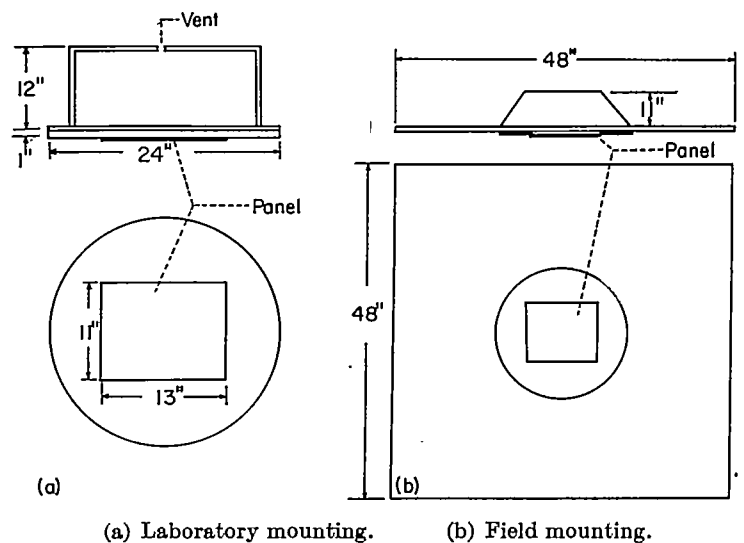For the determination of panel transfer characteristics and damping for which an intense discrete-frequency noise input was desired, the apparatus of figure 3 was used. This apparatus consisted of an air chopper or siren, which periodically interrupts an airstream to produce pressure pulsations. The siren is coupled by a short transition section to an acoustic horn with a length of 6 feet and a mouth diameter of 2 feet. The siren itself consists of a stator having 6 ports and 6 webs of equal width and a rotor of 6 ports of slightly less width. These rotor ports alternately cover and uncover the 6 stator ports at a rate determined by the speed of the rotor drive motor. The system was capable of generating sound levels up to 160 decibels at frequencies of 100 to 500 cycles per second.

INSTRUMENTATION

The measured data consisted mainly of panel stresses and frequencies and input pressure spectra. Figure 4 shows schematic diagrams of the instrument systems used to obtain these data. Figure 4 (a) shows the strain-gage setup. As is shown in figure 1, a Baldwin A–8 strain gage, which is roughly ⅛ inch long, was mounted at the middle of the short side of the panel in front of a bolt hole for all tests. A conventional strain-gage carrier and bridge system was used. Its output was channeled to a recording oscillograph for frequency observation and recording of time histories and to a thermocouple mean-square meter after filtering out the carrier with a 2,000 cycle per second low-pass filter. Calibration of the
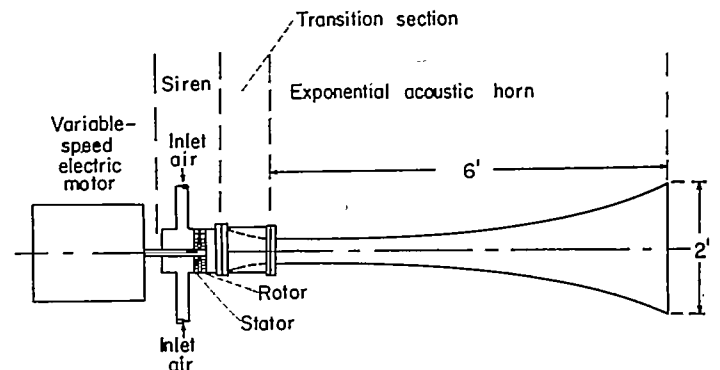

FIGURE 3.—Siren used in tests.

system for stress was made by statically loading a strain-gage cantilever beam and observing the oscillograph deflection and then assigning to that deflection the stress calculated for the system.

Figure 4 (b) shows schematically the instrumentation used for measurement of noise inputs. For periodic inputs (from the siren), the lower system of figure 4 (b) was used. It consisted of a dynamic-pressure gage, an associated carrier amplifier, and a panoramic frequency analyzer. Calibration of the system was made by comparison with a standard microphone of known sensitivity.

For random input, as from the 4-inch air jet and the turbojet engine, the system sketched at the top of figure 4 (b) was used. In this case a crystal microphone was used in conjunction with a tape recorder. For the spectrum analysis, playback of the tape records was made through a set of ⅓-octave filters. Since the results of such analyses depend upon the filter characteristics, they were corrected to spectrum-level values (band width of 1 cycle per second) from knowledge of the filter characteristics.

METHODS

In order to make calculations of stress for comparison with measured values, certain characteristics of the input acoustic loading and of the panel response were needed. For the loading, a representative spectrum of the pressure is involved; for the panels the determination of the static response to a given loading and the dynamic response to the equivalent sinusoidal loading is involved.

NOISE INPUTS

In all cases, for either periodic or random input, the input pressure that was used in calculations was measured at a

(a)

(b)

(a) Stress.
(b) Noise.

FIGURE 4.—Instrumentation used in panel tests.

point at the edge of the test panel. This practice was found to keep the measurement relatively free of the radiation field of the vibrating panel and results essentially in a value which corresponds to pressure at a rigid surface. Use of this pressure tacitly assumes unit correlation of pressure over the entire panel. This assumption seems to be justified for the fundamental frequencies of the panel models used in these tests as indicated by the correlation data of reference 3 for a similar engine. Further information on the noise pressure levels near turbojet engines is presented in reference 4 and in the appendix of this paper.

PANEL CHARACTERISTICS

In order to calculate the stress response to random noise, the static-stress response and the panel-admittance characteristics are needed. The frequency-response curves for each panel at various input-pressure levels were obtained by positioning the panel in its mount (either laboratory or field) about 1½ feet outside the mouth of the siren and operating the latter at constant output pressure and various frequencies. From the resulting stress response curves, damping and resonant frequency were obtained. All static stress curves were obtained with the panels in the laboratory mount by either evacuating or pressurizing the backing chamber to various levels.

METHOD OF STRESS ANALYSIS

As Miles (ref. 5) has shown, the problem of random excitation of a structural panel can be handled by a power-spectrum procedure in the following manner:

Consider that the panel behaves as a simple single-degree-of-freedom linear system. Its response to an input at frequency ω is determined by the square of its transfer function $1/Z(\omega)^2$ where

$$|Z(\omega)|^2 = \frac{1}{S_0^2}\left\{\left[1-\left(\frac{\omega}{\omega_0}\right)^2\right]^2 + 4\delta^2\left(\frac{\omega}{\omega_0}\right)^2\right\} \tag{1}$$

where
S_0 static stress per unit load
ω_0 resonant frequency
δ damping in terms of critical damping

If this system is excited by a random input which has the power spectrum $\Phi_N(\omega)$, the output stress response $\Phi_\sigma(\omega)$ is given as

$$\Phi_\sigma(\omega) = \frac{\Phi_N(\omega)}{|Z(\omega)|^2} \tag{2}$$

Integration of this relation throughout the width of the spectrum yields the following expression for the mean-square stress

$$\overline{\sigma^2} = \frac{\pi}{4\delta}\omega_0\Phi_N(\omega_0)S_0^2 \tag{3}$$

which is exact when the input spectrum is flat and is a good approximation for a system with low damping when the input spectrum is changing gradually in the vicinity of ω_0.

It is primarily with this latter relationship that the present report is concerned, inasmuch as measured stress data are
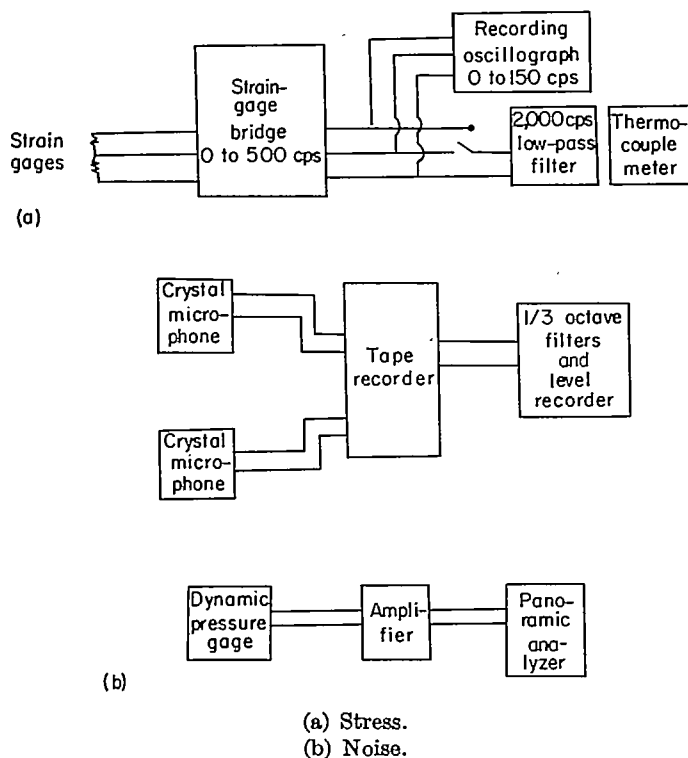
compared with values calculated from equation (3). In addition, it is proposed to apply this relationship, which assumes a strictly linear response, to panels which are driven into the nonlinear operating range and also to curved panels.

In addition to the root-mean-square stress response, there is interest also in the time history of stress, for this history undoubtedly affects fatigue life. As Miles discusses in reference 5, a linear single-degree-of-freedom system randomly excited is expected to respond at the natural frequency of the system and at stress amplitudes which vary as a function of time. The stress-amplitude envelope is expected to exhibit beats at more or less regular intervals and this condition was noted experimentally in reference 1. From the present tests, stress time histories were obtained at high random input levels where the panel response is somewhat nonlinear and also for the case where the loading spectrum contained a strong periodic component superposed on the random components.

Figure 5 presents sample stress time histories for various panels in the near noise field of the jet engine at the 100-percent engine-rotational-speed condition and at the afterburner condition. These sample stress records indicate the response frequency of the panels but the stress amplitudes as shown in the figure are not necessarily relative. At the 100-percent engine-rotational-speed condition of the engine, the noise inputs to the panels are essentially random in nature, whereas, for the afterburner condition, as is shown

in figure 6, an additional intense discrete-frequency component is present in the input spectrum. It can be seen that, for the 100-percent engine-rotational-speed condition, the stress responses for these three panels exhibit a beating which was noted experimentally in reference 1 for much lower random input levels.

However, in the afterburner case the records for the most part lack this characteristic beating. This is believed to reflect the presence of the strong periodic component in the loading spectrum. The 0.032-inch panel, which has a natural frequency almost coincident with the periodic afterburner component, responds almost sinusoidally as might be expected.

RESULTS AND DISCUSSION

NOISE INPUTS

The panels tested in this investigation were loaded randomly by the near sound fields of a 4-inch cold air jet and a turbojet engine operated at three thrust settings in order to have a range of input pressures. The turbojet settings were (1) afterburner, (2) 100-percent engine rotational speed, and (3) a condition estimated as 95-percent rotational speed. Figure 6 gives sample spectra from the engine for the 100-percent rotational speed and for the afterburner condition. These particular spectra apply to a position 31.4 feet downstream of the tailpipe and 1.58 feet from the 15° jet boundary. The overall sound levels associated with these spectra are in the range of 146 to 155 decibels.
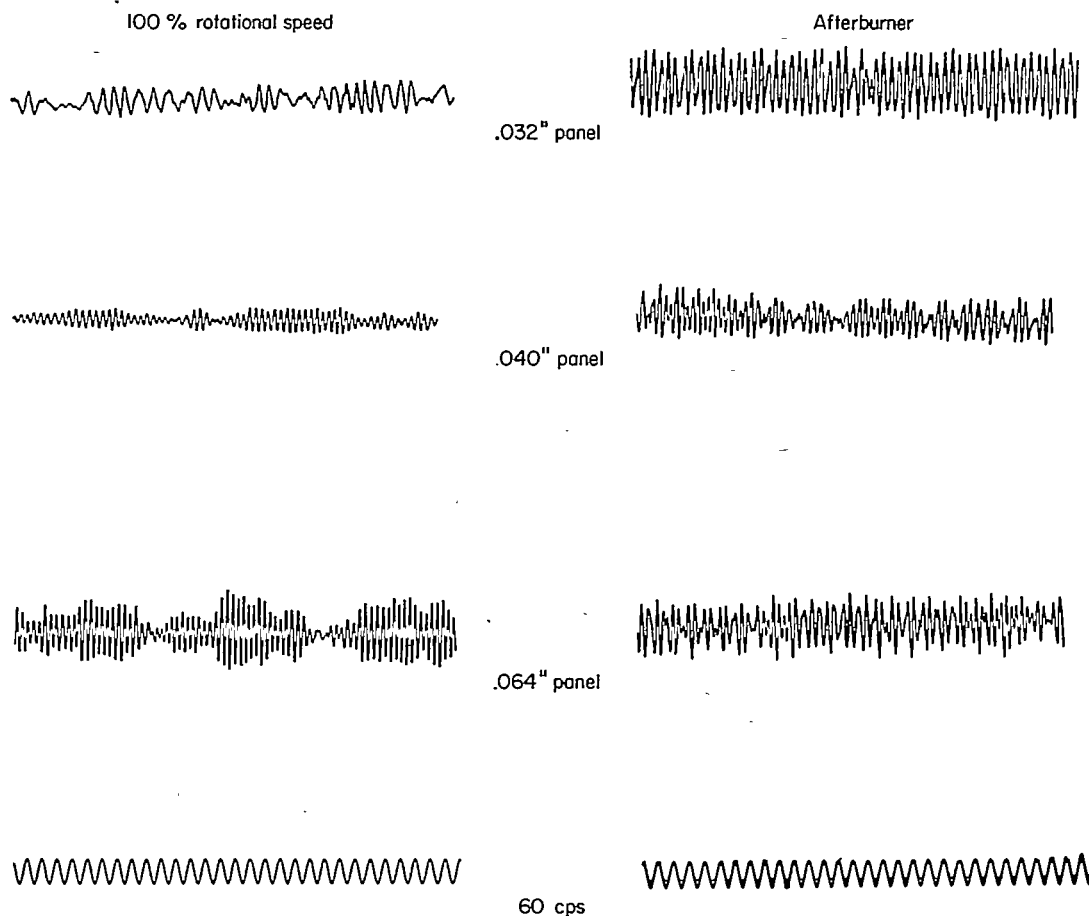

FIGURE 5.—Strain-gage response of panels to two different engine conditions.
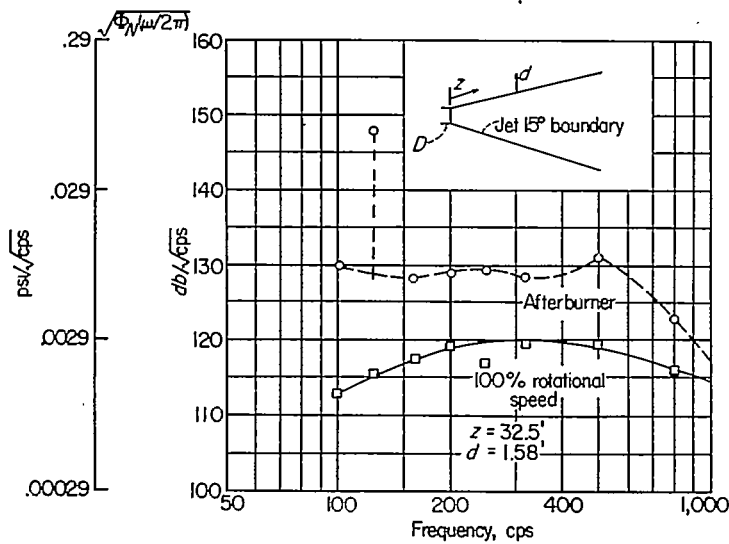
FIGURE 6.—Sample pressure spectra from the turbojet engine.

(a) Flat panel.
(b) Curved panel.

FIGURE 7.—Static stress characteristics of test panels.

The shapes of the spectrum curves are typical of those measured heretofore in the near field of turbojets (ref. 2) and the increment in pressure between the 100-percent engine rotational speed and the afterburner condition is about that expected on the basis that the near-field pressure varies as the square of the velocity. (See ref. 6.) In addition to this increase there is also noted a very intense discrete frequency component at 125 cycles per second. This component is attributed to a resonant condition in the tailpipe and has also been observed on some other engines. (See ref. 7.) This discrete frequency lies below the resonant frequencies of the 0.040-inch panel and the 0.064-inch panel and was nearly coincident with the resonant frequency of the 0.032-inch panel.

The spectra obtained with the turbojet at the estimated 95-percent rotational speed and with the 4-inch air jet had, in general, acoustic pressure distributions similar to those of figure 6, except that the levels were lower. More detailed information on the spatial distribution of pressure at various frequencies is given in the appendix. With the 4-inch jet, overall levels were in the range of 125 to 135 decibels; with the 95-percent engine rotational speed, overall levels were in the range of 135 to 145 decibels.

PANEL CHARACTERISTICS

Stress calculations obtained by using equation (3) require experimental values for several of the panel-response characteristics, namely, (1) the static response per unit input pressure, (2) the resonant frequency, and (3) the damping. Figures 7 to 10 present a summary of data of this type obtained from the panels tested.

Static stress response.—Figure 7 presents the static stress response for the various test panels. Figure 7(a) groups the data for the flat panels with thicknesses of 0.032 inch to 0.081 inch; figure 7(b) gives the static-stress values of the curved panels. Differentiation is made between loading with pressure and loading with a vacuum on the back side of the panels. As used in this paper, a positive stress is associated with a vacuum on the back side of the panel. Although the
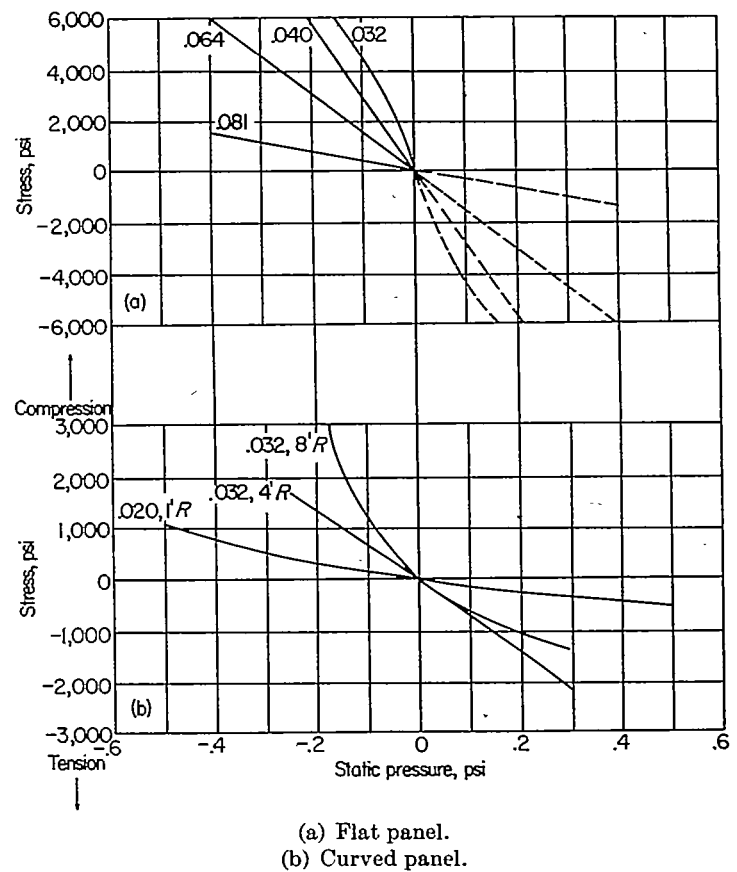
method of mounting allows slightly different bending moments for a given pressure or vacuum loading, the stress differences were found to be negligible for the flat panels in the range of test pressures shown. Figure 7(a) indicates a linear increase of stress with pressure loading for pressures up to at least 0.2 pound per square inch for all panels except the 0.032-inch panel, which was linear only up to about 0.05 pound per square inch.

In the case of the curved panels, the direction of loading is a significant factor, as indicated in figure 7 (b) where it can be seen that the slopes of the respective stress curves change more rapidly as a function of pressure.

Frequency-response characteristics.—From the tests with the siren, in which frequency was varied systematically while the acoustic input pressure to the panel was held constant at various levels, frequency-response curves were obtained for the flat and curved panels of various thicknesses.

Figure 8 presents sample results for a flat panel of 0.040-inch thickness at three different input pressures. Peak stress amplitude in pounds per square inch is plotted as a function of driving frequency in cycles per second for root-mean-square values of fundamental siren pressure of 0.00184, 0.00366, and 0.0147 pound per square inch. At the lowest input pressure the response is fairly symmetrical about the resonant frequency which at that pressure is 148 cycles per second. This type of response is typical of a linear system. As the input pressure is increased to 0.00366 pound per square inch, the response curve takes on a skewed form, the peak now occurring at 163 cycles per second. As shown in reference 8 this increase in pressure reflects nonlinearities
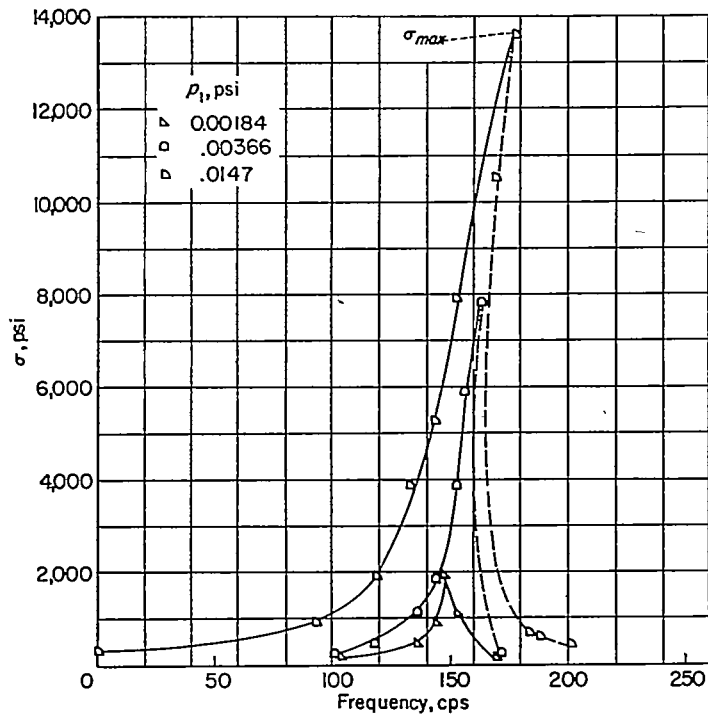
FIGURE 8.—Frequency-response characteristics of flat panels.
$t=0.040$ inch.

of the system whereby the stiffness is increasing with panel deflections. Experimentally this type of response results in a triple-valued curve for a certain frequency range within which the curve is very difficult to define. For that reason a portion of the response curve is shown by a dashed line. At the input pressure of 0.0147 pound per square inch, the skewness is even more evident and the peak occurs at a still higher frequency.

The trends illustrated in figure 8 were found to be generally representative of all the flat panels tested, except, of course, that the resonant frequencies are higher for thicker panels.

Figure 9 presents similar results for a curved panel with a thickness of 0.032 inch and a radius of curvature of 4 feet. Response curves for input pressures of 0.00114, 0.0114, and
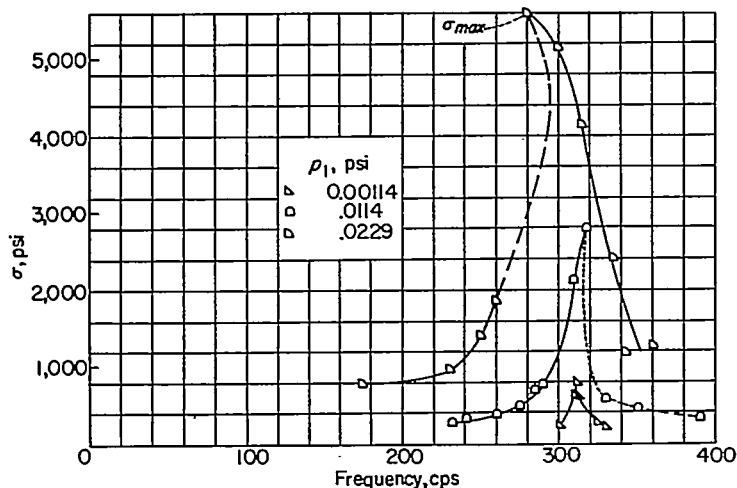
0.0229 pound per square inch are given. As was the case with flat panels, the curved-panel response is very nearly symmetrical about resonance at the lowest pressure and tends to skew to the right at intermediate pressures. Unlike the flat panels, however, the curved panel assumes a response which skews to the left at the highest pressures. As shown in reference 8, this type of nonlinear response is associated with a condition of decreasing stiffness with deflection increase. For a curved panel this condition is probably due to the tendency for the panel to dimple inward in response to a pressure on its convex surface.

Damping.—As is well known, either the height of the frequency-response curve or its width at the half-power points provides an indication of the panel damping. However, because of the unstable range involved just above or below the resonance of a nonlinear panel, the width is very difficult to obtain experimentally. Thus all damping data presented were obtained from the resonant amplification:

$$\delta = \frac{\sigma_{st}}{2(\sigma_{max})\omega_0}$$

Figure 10 illustrates the variation of damping δ as a function of the root-mean-square value of panel stress for flat panels of thickness 0.040 inch, 0.064 inch, and 0.081 inch. All data points shown are obtained from the resonant response of the panel in question at a particular level of acoustic pressure. In general, for the field mount it can be seen that at the higher stress conditions the damping increases very rapidly with stress (or deflection). Also apparent is some tendency for the damping to increase again at very low stresses. The reason for this increase is not known; however, this tendency was also apparent in the earlier tests (ref. 1) in which only low levels of excitation were employed.

The fact that the experimental points for all thicknesses tested fall on a common curve is a probable indication that, for the range of panel thicknesses tested, damping is primarily dependent upon stress level. The average damping curve for flat panels of 0.040 inch, 0.064 inch, and 0.081

FIGURE 9.—Frequency-response characteristics of curved panels.
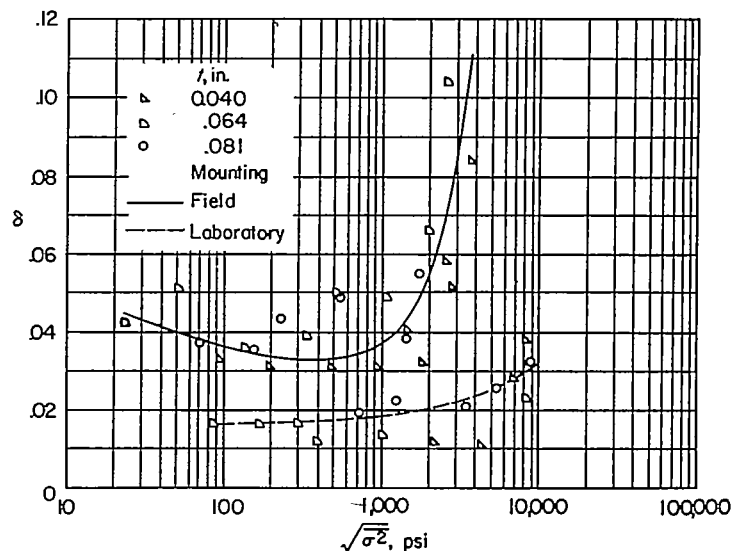$t=0.032$; $R=4$ feet.

FIGURE 10.—Damping characteristics of flat panels.

inch in the laboratory mount is given by the dashed curve. (See fig. 10.) This curve illustrates clearly the significance of the mounting conditions since the laboratory mount with its less absorptive backing material yields appreciably lower values of damping. Damping for the curved panels was found to vary only slightly from that of the flat panels at the high stresses encountered with turbojet excitation.

PROCEDURE FOR CALCULATING STRESS

The success in using equation (3) to predict stress due to a random input depends to a large extent on the use of experimentally determined quantities. In order to facilitate these calculations, equation (3) can be rewritten as follows:

$$\sqrt{\Phi_N(\omega_0)} = \sqrt{\sigma^2}\left(\frac{4\delta}{\pi\omega_0 S_0^2}\right)^{1/2}$$

where the quantities in parentheses have been shown to be a function of the stress level of the panel.

A curve of stress as a function of input acoustic pressure can be determined by solving the above equation for $\sqrt{\Phi_N\left(\frac{\omega_0}{2\pi}\right)}$ by using arbitrary values of $\sqrt{\sigma^2}$ and the corresponding experimentally determined values of δ, S_0, and ω_0.

The data of figures 7, 8, 10, and 11 are used in conjunction with equation (3) to determine the curve of root-mean-square stress as a function of jet acoustic pressure $\sqrt{\Phi_N\left(\frac{\omega_0}{2\pi}\right)}$ shown in figure 12. For a given root-mean-square stress level, the value of S_0 is determined from figure 7 by using the relation

$$\sigma_{st} = 2\delta\sqrt{2}\sqrt{\sigma^2}$$

The damping δ at the appropriate stress level is obtained directly from the curves of figure 10. The natural frequency ω_0 is obtained from the response-curve data (such as that given in fig. 8) used in determining damping.

In addition to figures 7, 8, and 10, curves of mean-square stress as a function of siren acoustic pressure such as those
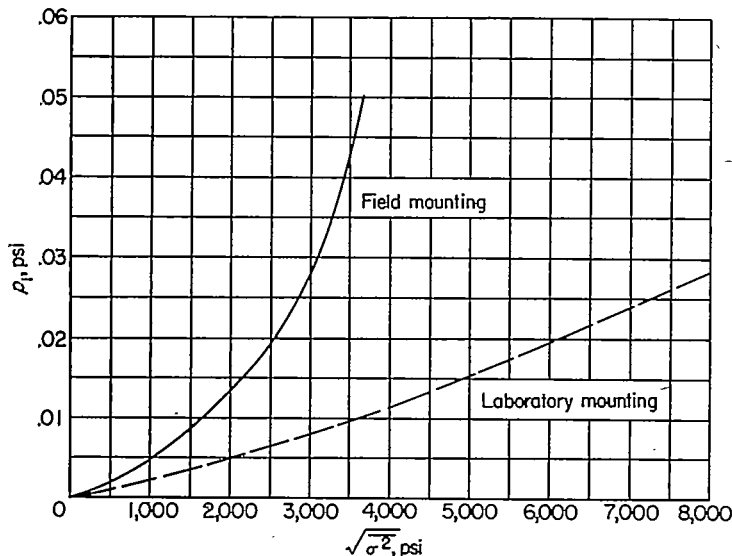
FIGURE 11.—Siren pressure as a function of root-mean-square stress for a 0.064-inch panel.
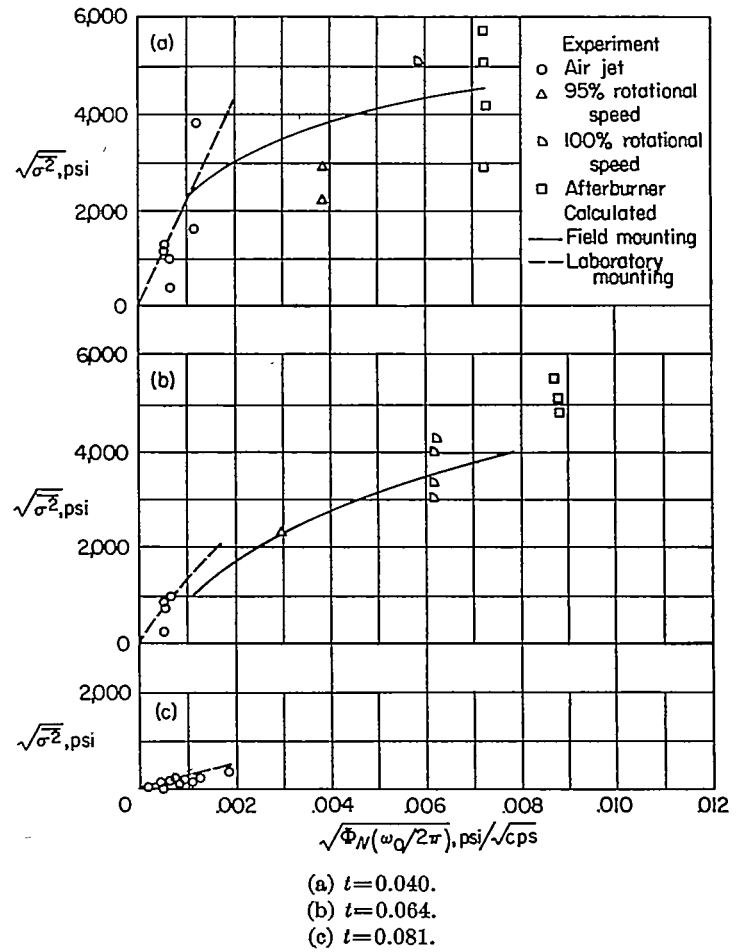
(a) $t = 0.040$.
(b) $t = 0.064$.
(c) $t = 0.081$.

FIGURE 12.—Comparison of calculated and measured stresses for flat panels.

of figure 11 are useful in the calculation of $\sqrt{\Phi_N\left(\frac{\omega_0}{2\pi}\right)}$ when S_0 is in the nonlinear range. These curves are constructed from figure 7 and the average stress-damping curves of figure 10. For a given root-mean-square stress level, the associated siren acoustic pressure is first determined from a curve such as figure 11. The quantity S_0 was taken as the slope of a secant line drawn between two points on the curve of figure 7 at the appropriate pressure levels $\pm\sqrt{2}p_1$.

COMPARISON OF CALCULATED AND MEASURED STRESSES

A comparison of the measured and calculated stresses for flat panels of 0.032 inch, 0.040 inch, 0.064 inch, and 0.081 inch and for curved panels of 0.032 inch with radii of 8 feet and 4 feet is given in figures 12 and 13. Figure 12 relates to flat panels and presents calculated and measured root-mean-square stresses as a function of input spectrum-level pressure $\sqrt{\Phi_N\left(\frac{\omega_0}{2\pi}\right)}$ for thicknesses of 0.040 inch, 0.064 inch, and 0.081 inch. In each case the curve represents the calculated stress variation and the points are measured stress values from tests with both the 4-inch laboratory air jet and the turbojet.

For the 0.040-inch panel, the calculated and measured stresses are found to be in very good agreement at low pressures and the theory seems to be generally conservative
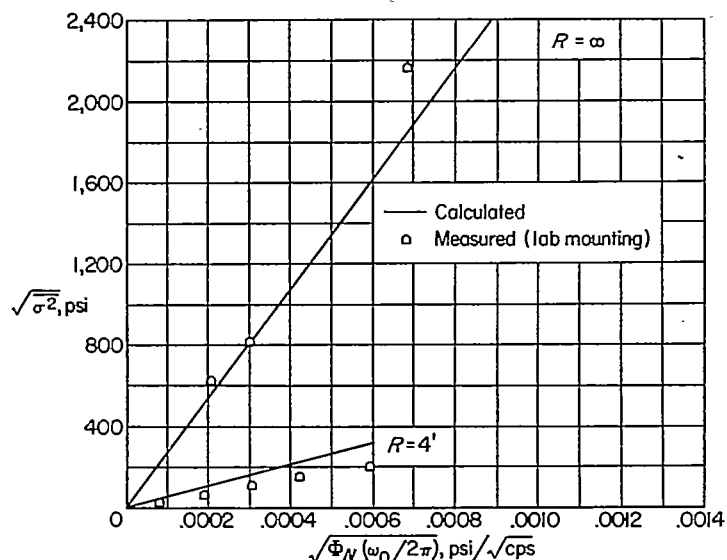
FIGURE 13.—Effect of curvature on calculated and measured stress of 0.032-inch 2024–T3 panels.

at the higher pressures. For the 0.081-inch panel only low-pressure data were obtained, but over the range tested the calculated and measured values are in excellent agreement. Thus it appears from figure 12 that equation (3) will yield stress values which are in fairly good agreement with measured values on flat panels over a wide range of input pressures and for a doubling of panel thickness.

The fact that the analysis is in such good agreement with experimental results for both the 4-inch air jet and the turbojet engine seems to indicate that the correlation length is a function of frequency and not of jet size.

Figure 13 compares calculated and measured stresses for a panel of given thickness (0.032 inch) having different radii of curvature. Again the root-mean-square stress $\sqrt{\overline{\sigma^2}}$ is plotted as a function of root-mean-square spectrum-level

pressure $\sqrt{\Phi_N\!\left(\dfrac{\omega_0}{2\pi}\right)}$. The upper curve and associated points allow comparison of calculated and measured stresses for a flat panel ($R=\infty$). The agreement is similar to that of figure 12 for thicker panels, although the pressure range for the 0.032-inch panels is more limited. As the radius of curvature is decreased to 4 feet, the agreement between calculated and measured stresses is still rather good, the theory being consistently conservative.

CONCLUSIONS

An investigation was made of the stress response of simple flat and curved rectangular panels to random acoustic noise. In addition, this stress response was calculated by using general harmonic-analysis methods. This investigation indicated the following conclusions:

1. At input pressures of the order of those encountered in full-scale configurations, the panels are somewhat nonlinear. With flat panels this nonlinearity involves a stiffening spring constant; with curved panels the nonlinearity involves a decreasing spring constant.

2. Within reasonable limits in the stress range of the tests, the combined structural and radiation damping of flat panels is independent of panel thickness and depends only upon panel stress or deflection. Damping increases rapidly with stress at the higher stresses.

3. The generalized harmonic analysis predicts stresses which are in fair agreement with measured values for flat panels and for curved panels of radius 4 feet over the range of input pressures tested.

LANGLEY AERONAUTICAL LABORATORY,
NATIONAL ADVISORY COMMITTEE FOR AERONAUTICS,
LANGLEY FIELD, VA., *June 3, 1957.*

APPENDIX

NEAR NOISE FIELD OF THE TURBOJET ENGINE

Because of the rather limited near-field noise data from full-scale turbojets, particularly for afterburning conditions, it seems advisable to include more detailed results of the survey taken with an engine. The near field was explored along lines parallel to the theoretical 15° jet boundary at radial distances of 0.79 foot, 1.58 feet, and 3.16 feet for the engine under 100-percent rotational-speed conditions and for afterburner operation. The thrust and nozzle diameters for the 100-percent rotational-speed and for the afterburner conditions were 2,780 pounds at 15.38 inches and 3,390 pounds at 17.5 inches, respectively. In addition, data from another turbojet engine were obtained at a power condition estimated to be at 95-percent rotational speed for a thrust of approximately 2,300 pounds and a nozzle diameter of 15.38 inches. Figures 14 and 15 present some of the results obtained.

Figure 14 includes a plot of overall sound pressure as a function of slant distance z for 100-percent rotational-speed and afterburner conditions of the engine. Radial distances of 0.79 foot, 1.58 feet, and 3.16 feet are given for afterburner operation and radial distances of 1.58 feet and 3.16 feet are given for the 100-percent rotational-speed condition. In general, these curves indicate that the largest pressures occur farther downstream of the tailpipe as the radial distance is increased. This result is in agreement with the model-jet trends reported in reference 6. Also apparent is the fact that, at stations just downstream of the nozzle, the pressures decrease very rapidly with radial distance; whereas, at stations farther downstream there is only a slight decrease of pressure with radial distance. Comparison of the afterburner and 100-percent rotational-speed curves shows that operation of the afterburner increases the pressure fluctuations by as much as a factor of 5 in some locations. Of course, this particular engine is somewhat unique in that (as discussed previously) it resonates during afterburning and the periodic noise of that origin dominates the spectrum, particularly at stations near the tailpipe.

Figures 15 (a), 15 (b), and 15 (c) illustrate the spatial distribution of spectrum-level pressure at various frequencies
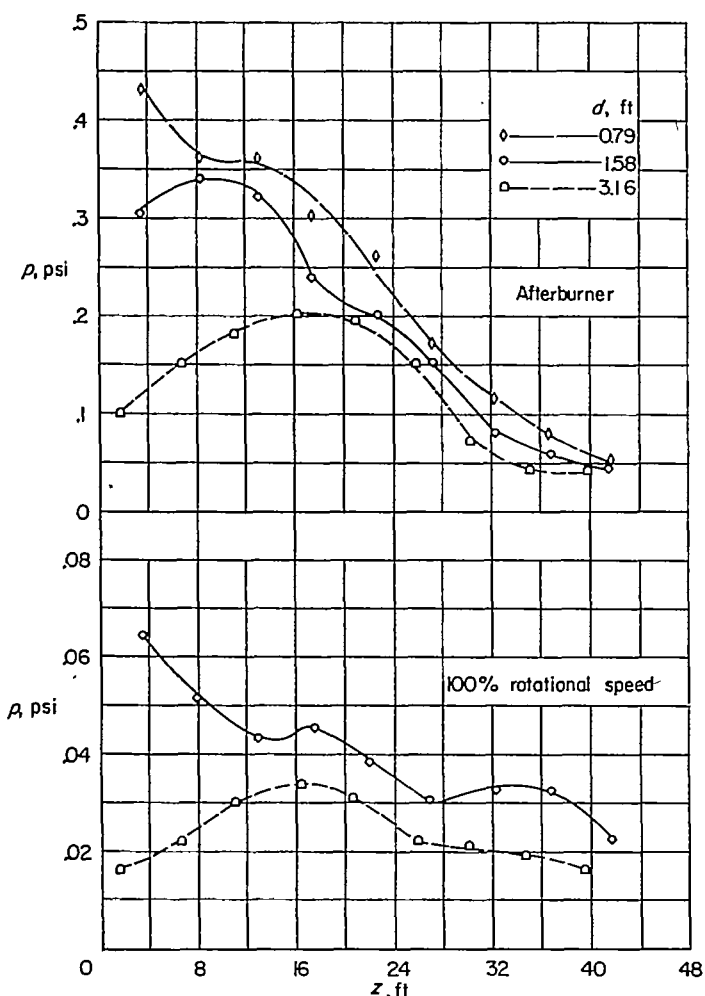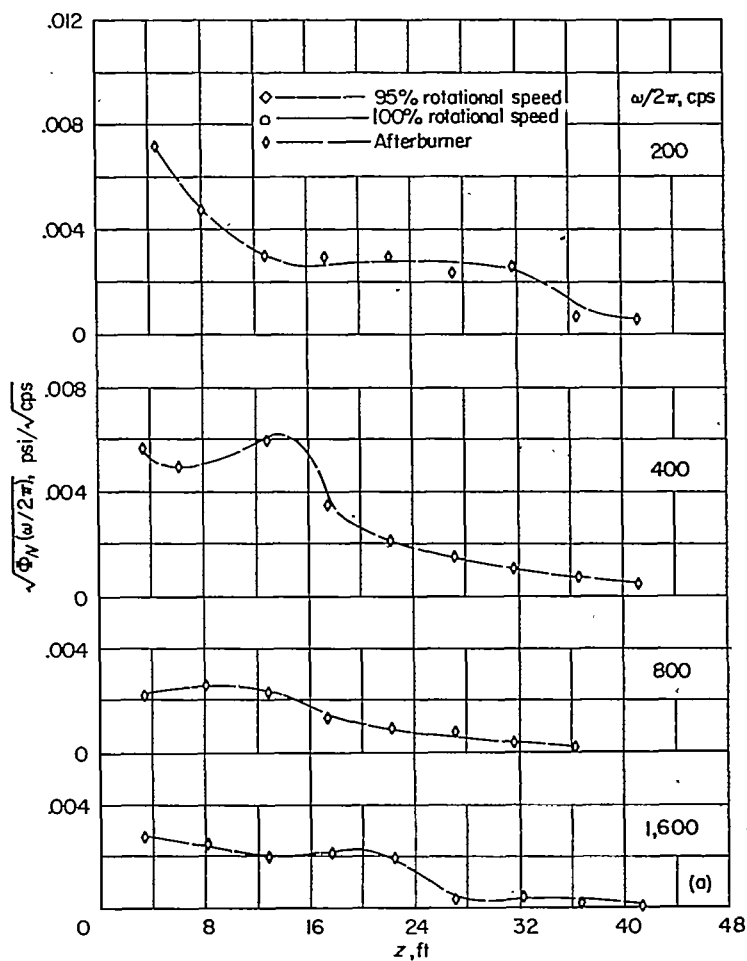

FIGURE 14.—Overall near-field sound pressures at various axial and radial distances from the turbojet engine.

(a) $d = 0.79$ foot.

FIGURE 15.—Near-field sound pressures of the turbojet engine at various frequencies as a function of axial and radial distances.
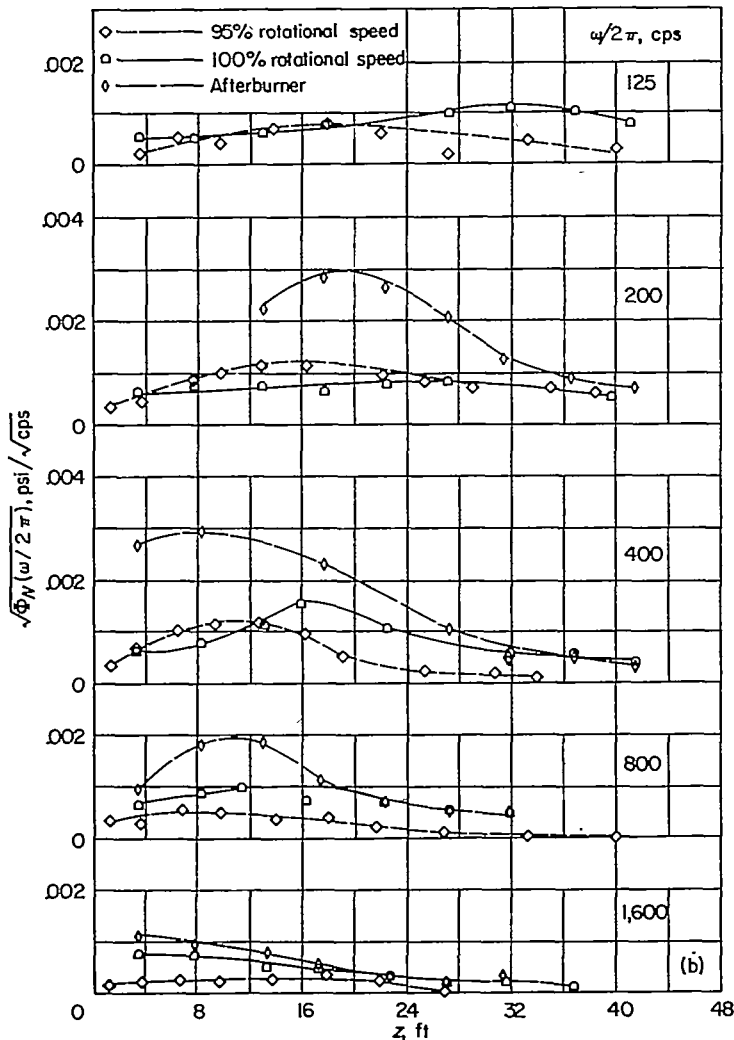
(b) $d=1.58$ feet.

FIGURE 15.—Continued.

(c) $d=3.16$ feet.

FIGURE 15.—Concluded.

for radial distances of 0.79 foot, 1.58 feet, and 3.16 feet, respectively. Figure 15 (a), for $d=0.79$ foot, presents only data from afterburner operation; figures 15 (b) and 15 (c) include data at the 95-percent and 100-percent rotational-speed conditions.

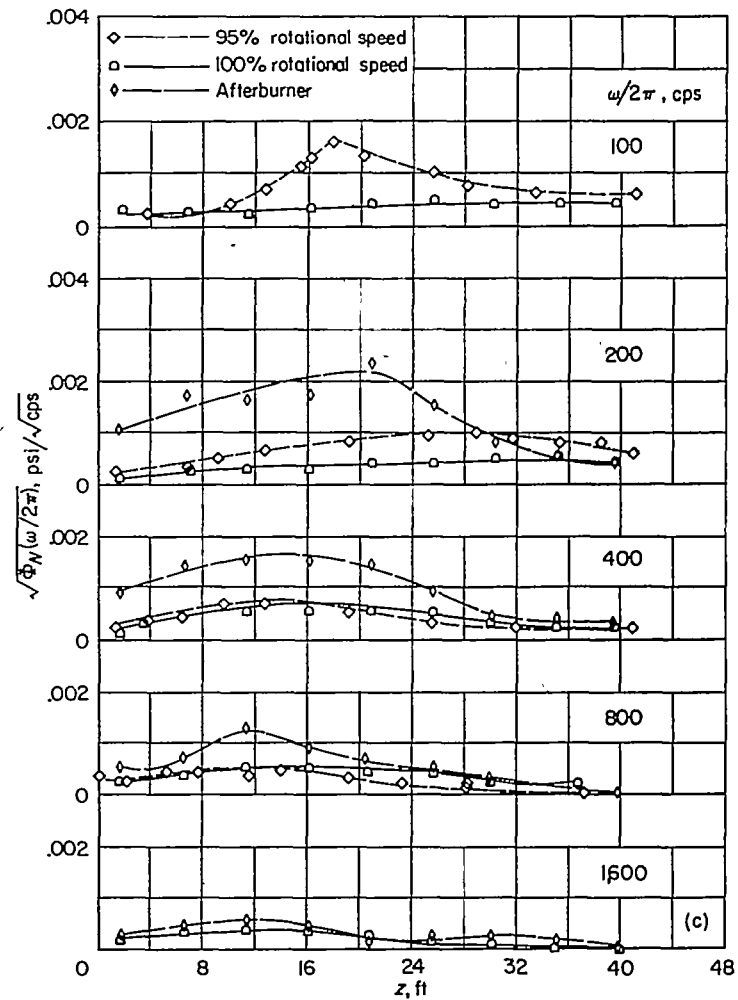In general, these results indicate that the maximum pressure at a given frequency occurs at some distance downstream of the tailpipe. As the engine rotational speed (and thus jet velocity) is increased, the point of maximum pressure for any given frequency tends to occur somewhat near the tail pipe. Similarly, the high-frequency components tend to have maximum pressure values nearer the tailpipe than the low-frequency components. As shown in reference 6, this result is also in agreement with near-field results from un heated model jets.

REFERENCES

1. Hess, Robert W., Lassiter, Leslie W., and Hubbard, Harvey H.: A Study of the Response of Panels to Random Acoustic Excitation. NACA RM L55E13c, 1955.

2. Lassiter, Leslie W., Hess, Robert W., and Hubbard, Harvey H.: An Experimental Study of the Response of Simple Panels to Intense Acoustic Loading. Jour. Aero. Sci., vol. 24, no. 1, Jan. 1957, pp. 19–24, 80.

3. Callaghan, Edmund E., Howes, Walton L., and Coles, Willard D. (with appendix by Channing C. Conger and Donald F. Berg): Near Noise Field of a Jet-Engine Exhaust. II. Cross Correlation of Sound Pressures. NACA TN 3764, 1956.

4. Howes, Walton L., and Mull, Harold R.: Near Noise Field of a Jet-Engine Exhaust. I. Sound Pressures. NACA TN 3763 1956.

5. Miles, John W.: On Structural Fatigue Under Random Loading Jour. Aero. Sci., vol. 21, no. 11, Nov. 1954, pp. 753–762.

6. Lassiter, Leslie W., and Hubbard, Harvey H.: The Near Noise Field of Static Jets and Some Model Studies of Devices for Noise Reduction. NACA Rep. 1261, 1956. (Supersedes NACA TN 3187.)

7. Lassiter, Leslie W.: Noise From Intermittent Jet Engines and Steady-Flow Jet Engines With Rough Burning. NACA TN 2756, 1952.

8. Den Hartog, J. P.: Mechanical Vibrations. Second ed., McGraw Hill Book Co., Inc., 1940.